ICAST2014: 25nd International Conference on Adaptive Structures and Technologies
October 6-8th, 2014, The Hague, The Netherlands

ICAST2014 # 040

Development of a Nonlinear Multimodal Energy Harvester with Magnetic Coupling

Hongyan WANG[1], Louise WAN[2], Kirsten LY[3], and Lihua TANG[4*]

[1] College of Computer and Control Engineering, Qiqihar University, Qiqihar City, P.R. China
[2,3,4] Department of Mechanical Engineering, University of Auckland, New Zealand

Abstract

One main concern in vibration energy harvesting is the operating bandwidth of the harvesters. The random and time-varying nature of most vibration sources requests research efforts to improve the bandwidth of vibration energy harvesters. Many attempts have been made to address this issue in the past few years. Efforts include exploiting multimodal structures and nonlinear configurations. These concepts have yielded some exciting results. Hybrid configurations combining these ideas are expected to provide an even better operating bandwidth and yet to be investigated. This paper proposes a nonlinear two degree of freedom (2DOF) piezoelectric energy harvester (PEH) with magnetic coupling, in which a linear parasitic oscillator attached to the main energy harvesting component is exploited for two resonant peaks and the magnetic coupling for nonlinear dynamics, thus to achieve the broad bandwidth. A nonlinear electromechanical model is established for numerical simulation. Parametric studies are conducted subsequently on various magnetic configurations and parasitic oscillator configurations. The results indicate that the monostable nonlinear configuration can achieve two significant peaks close to each other with properly tuned magnetic coupling and linear oscillator. The tuned monostable 2DOF PEH configuration is advantageous over the optimal linear 2DOF PEH in terms of two higher peak outputs and wider bandwidth thanks to the nonlinear dynamics. On the other hand, though there might be only one peak contributing to energy harvesting and the oscillations are confined in one potential well, the enhanced peak output and widened bandwidth make the bistable 2DOF PEH still attractive.

1. INTRODUCTION

The use of the conventional batteries in low-power electronics, such as wireless sensors, has the limitations in terms of their lifespans and the subsequent costly replacement in practical structural monitoring, machine condition monitoring and medical implant devices. Ambient vibrations can be harnessed for generating electricity and thus provide a potential solution for self-sustained wireless sensing applications. A conventional vibration energy harvester is a linear one degree of freedom (1DOF) model consisting of a spring-mass system with an electrostatic, piezoelectric or electromagnetic transducer. The linear 1DOF harvester can only effectively collect energy within a narrow bandwidth. With a slight shift from resonant frequency, the performance of the harvester will decrease drastically. The random and

*Corresponding author, email: l.tang@auckland.ac.nz

time-varying nature of most vibration sources demands the efforts to improve the operating bandwidth of the vibration energy harvesters.

Many attempts have been made to address the bandwidth issue of vibration energy harvesting in the past few years. One promising method is to design multimodal energy harvesting structures. The multimodal structures take advantage of multiple resonant frequencies, which can harvest useful power over multiple frequency spectra. Some researchers proposed multimodal energy harvesters based on 2DOF configurations, including L-shaped beam structure [1], 2DOF cut-out beam [2], 2DOF hybrid piezoelectric-electromagnetic energy harvester [3], energy harvesters with dynamic magnifiers or dynamic oscillators [4-7], and dual mass structures [8, 9]. Other researchers propose the plate structure [10] and fractal-inspired structure [11] for multimodal responses. It has been demonstrated that with properly selected parameters, it is possible to achieve multiple close resonant peaks with significant output at each peak [7].

Another promising method for broadband energy harvesting is to exploit the nonlinear dynamics. A nonlinear vibration energy harvester can be easily developed by introducing the magnetic force. Either monostable or bistable response can be achieved using different magnetic configurations. Stanton et al. [12] proposed a monostable harvester in which both the hardening and softening responses could occur by tuning the magnetic interactions. Erturk et al. [13] investigated the bistable mechanism of a broadband piezo-magnetoelastic generator. Tang et al. [14] experimentally studied the monostable and bistable configurations under sinusoidal and random vibrations with various excitation levels. The optimal nonlinear configuration is determined to be near the monostable to bistable transition region. All these investigations have demonstrated the exciting potential of exploiting nonlinear dynamic structures to enlarge the operating bandwidth of energy harvesting.

This paper proposes a nonlinear 2DOF PEH with magnetic coupling, which combines the concepts of multimodal and nonlinear techniques to further widen the operating bandwidth. The magnetic coupling with the main energy harvesting structure introduces the nonlinearity to the system and a linear parasitic oscillator is attached to the main structure to achieve two resonant peaks. A nonlinear electromechanical model of 2DOF PEH is established. The effects of both the distance between two repulsive magnets (the strength of magnetic coupling and nonlinearity) and the mass of the parasitic oscillator on the resonant peaks of the nonlinear 2DOF PEH are investigated. The monostable and bistale responses are obtained and compared with their optimal linear 2DOF counterpart.

2. ELECTROMECHANICAL MODELS

In this section, we established the electromechanical lumped parameter model of the nonlinear 2DOF PEH, together with a brief introduction of the conventional linear 2DOF PEH. Parametric studies can then be performed to evaluate its performance in terms of the resonant frequencies, displacements and electrical outputs.

2.1 Linear 2DOF Harvester

Figure 1 shows a conventional linear 2DOF PEH model [7]. The mass m_1, spring k_1 and damping component η_1, are connected to the base. The piezoelectric element is placed between the base and m_1. Hence, m_1, k_1, η_1 and the piezoelectric element form the energy harvesting component of the system. The mass m_2, spring k_2 and damping component η_2, which form a parasitic oscillator, are attached to m_1. As the base is excited sinusoidally, the piezoelectric element generates alternating electrical outputs and delivers the power to the resistor R. u_0, u_1 and u_2 are the absolute displacement of the base, m_1 and m_2, respectively.

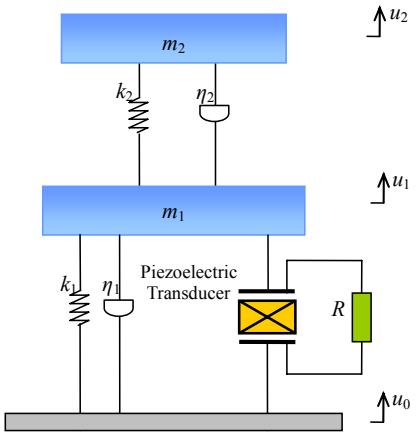

Figure 1. Linear 2DOF PEH model [7]

The governing equations of the linear 2DOF PEH model can be written as

$$\begin{cases} m_1\ddot{u}_1 = -\eta_1\left(\dot{u}_1-\dot{u}_0\right)-k_1\left(u_1-u_0\right)-\theta V+\eta_2\left(\dot{u}_2-\dot{u}_1\right)+k_2\left(u_2-u_1\right) \\ m_2\ddot{u}_2 = -\eta_2\left(\dot{u}_2-\dot{u}_1\right)-k_2\left(u_2-u_1\right) \\ -\theta\left(\dot{u}_1-\dot{u}_0\right)+C^S\dot{V}+V/R=0 \end{cases} \tag{1}$$

where C^S is the capacitance of the piezoelectric element; θ is the electromechanical coupling coefficient and; V is the voltage output across R. Equation (1) can be rearranged as

$$\begin{cases} m_1\left(\ddot{u}_1-\ddot{u}_0\right)+\eta_1\left(\dot{u}_1-\dot{u}_0\right)+k_1\left(u_1-u_0\right)+\theta V-\eta_2\left(\dot{u}_2-\dot{u}_1\right)-k_2\left(u_2-u_1\right)=-m_1\ddot{u}_0 \\ m_2\left(\ddot{u}_2-\ddot{u}_1\right)+\eta_2\left(\dot{u}_2-\dot{u}_1\right)+k_2\left(u_2-u_1\right)=-m_2\left(\ddot{u}_1-\ddot{u}_0\right)-m_2\ddot{u}_0 \\ -\theta\left(\dot{u}_1-\dot{u}_0\right)+C^S\dot{V}+V/R=0 \end{cases} \tag{2}$$

Setting $y=u_2-u_1$, $x=u_1-u_0$, equation (2) can be written as

$$\begin{cases} m_1\ddot{x}+\eta_1\dot{x}+k_1x+\theta V-\eta_2\dot{y}-k_2y=-m_1\ddot{u}_0 \\ m_2\ddot{y}+\eta_2\dot{y}+k_2y=-m_2\ddot{x}-m_2\ddot{u}_0 \\ -\theta\dot{x}+C^S\dot{V}+V/R=0 \end{cases} \tag{3}$$

Equation (3) can be further rearranged as

$$\begin{cases} m_1\ddot{x}+\eta_1\dot{x}+k_1x+\theta V-\eta_2\dot{y}-k_2y=-m_1\ddot{u}_0 \\ m_2\ddot{y}+\left(1+\dfrac{m_2}{m_1}\right)\left(\eta_2\dot{y}+k_2y\right)-\dfrac{m_2}{m_1}\left(\eta_1\dot{x}+k_1x+\theta V\right)=0 \\ -\theta\dot{x}+C^S\dot{V}+V/R=0 \end{cases} \tag{4}$$

Let $u=m_2/m_1$ and define the state space vector

$$\left[q(1)\ q(2)\ q(3)\ q(4)\ q(5)\right]^T=\left[x\ \dot{x}\ y\ \dot{y}\ V\right]^T \tag{5}$$

the governing equations of the linear 2DOF PEH can be written in the state space form as

$$\begin{bmatrix} \dot{q}(1) \\ \dot{q}(2) \\ \dot{q}(3) \\ \dot{q}(4) \\ \dot{q}(5) \end{bmatrix} = \begin{bmatrix} q(2) \\ -\omega_1^2 q(1) - 2\zeta_1\omega_1 q(2) + u\left(\omega_2^2 q(3) + 2\zeta_2\omega_2 q(4)\right) - \dfrac{1}{m_1}\theta q(5) - \ddot{u}_0 \\ q(4) \\ \omega_1^2 q(1) + 2\zeta_1\omega_1 q(2) - (u+1)\left(\omega_2^2 q(3) + 2\zeta_2\omega_2 q(4)\right) + \dfrac{1}{m_1}\theta q(5) \\ \dfrac{\theta}{C^S} q(2) - \dfrac{q(5)}{C^S R} \end{bmatrix} \tag{6}$$

where $\omega_1 = \sqrt{k_1/m_1}$, $\omega_2 = \sqrt{k_2/m_2}$, $\zeta_1 = \eta_1 \Big/ \left(2\sqrt{k_1 m_1}\right)$, $\zeta_2 = \eta_2 \Big/ \left(2\sqrt{k_2 m_2}\right)$

2.2 Nonlinear 2DOF Harvester with Magnetic Coupling

Nonlinear dynamics can be easily achieved by introducing magnetic coupling. In this paper, we propose a nonlinear 2DOF PEH model with the magnetic coupling, which combines the nonlinear technique and multimodal technique in an energy harvesting system to enlarge its operating bandwidth. Figure 2(a) shows the proposed nonlinear 2DOF PEH model where the magnetic force F_{mag} is applied to the mass m_1. Figure 2(b) illustrates the potential implementation of the nonlinear 2DOF PEH, which comprises a piezoelectric beam with a tip magnetic mass interacting with a magnet fixed to the base and a small parasitic beam oscillator. The parasitic beam oscillator is used to introduce two resonant peaks. The magnetic coupling is used to tune the resonant peaks and introduce the nonlinear dynamics. As two magnets approach to each other (decreasing the distance D between the two magnets), nonlinear behaviors appear and the response curves are bent.

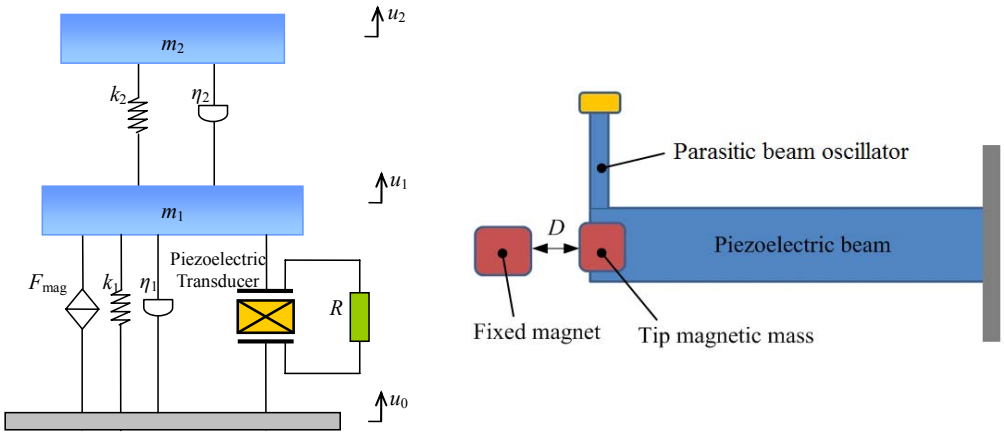

(a) (b)

Figure 2. (a) Proposed nonlinear 2DOF PEH model (b) Potential implementation

A magnetic dipole-dipole interaction is assumed throughout this paper and the potential energy induced by the magnets can be expressed as

$$U_{\text{mag}}(x)=\frac{\mu_0\sigma_1\sigma_2}{2\pi}\left(x^2+D^2\right)^{-\frac{3}{2}} \tag{7}$$

where μ_0 is the permeability constant; σ_1 and σ_2 are the effective magnetic moments of the two magnets. The derivation of the potential energy provides the magnetic force as

$$F_{\text{mag}}(x)=-\frac{3\mu_0\sigma_1\sigma_2 x}{2\pi}\left(x^2+D^2\right)^{-\frac{5}{2}} \tag{8}$$

Including the magnetic force, the governing equations of the nonlinear 2DOF PEH model is written as

$$\begin{cases} m_1\ddot{u}_1=-\eta_1\left(\dot{u}_1-\dot{u}_0\right)-k_1\left(u_1-u_0\right)-\theta V+\eta_2\left(\dot{u}_2-\dot{u}_1\right)+k_2\left(u_2-u_1\right)+F_{\text{mag}} \\ m_2\ddot{u}_2=-\eta_2\left(\dot{u}_2-\dot{u}_1\right)-k_2\left(u_2-u_1\right) \\ -\theta\left(\dot{u}_1-\dot{u}_0\right)+C^S\dot{V}+V/R=0 \end{cases} \tag{9}$$

Setting $y=u_2-u_1$, $x=u_1-u_0$, and rearranging equation (9) yields

$$\begin{cases} m_1\ddot{x}+\eta_1\dot{x}+k_1x+\theta V-\eta_2\dot{y}-k_2y-F_{\text{mag}}=-m_1\ddot{u}_0 \\ m_2\ddot{y}+\left(1+\dfrac{m_2}{m_1}\right)\left(\eta_2\dot{y}+k_2y\right)-\dfrac{m_2}{m_1}\left(\eta_1\dot{x}+k_1x+\theta V-F_{\text{mag}}\right)=0 \\ -\theta\dot{x}+C^S\dot{V}+V/R=0 \end{cases} \tag{10}$$

Letting $u=m_2/m_1$ and defining the same state space vector as equation (5), the governing equations of the nonlinear 2DOF PEH can be written in the state space form as

$$\begin{bmatrix} \dot{q}(1) \\ \dot{q}(2) \\ \dot{q}(3) \\ \dot{q}(4) \\ \dot{q}(5) \end{bmatrix}=\begin{bmatrix} q(2) \\ -\omega_1^2q(1)-2\zeta_1\omega_1q(2)+u\left(\omega_2^2q(3)+2\zeta_2\omega_2q(4)\right)-\dfrac{1}{m_1}\left(\theta q(5)-F_{\text{mag}}\right)-\ddot{u}_0 \\ q(4) \\ \omega_1^2q(1)+2\zeta_1\omega_1q(2)-(u+1)\left(\omega_2^2q(3)+2\zeta_2\omega_2q(4)\right)+\dfrac{1}{m_1}\left(\theta q(5)-F_{\text{mag}}\right) \\ \dfrac{\theta}{C^S}q(2)-\dfrac{q(5)}{C^SR} \end{bmatrix} \tag{11}$$

3. PARAMETRIC STUDY AND RESULTS

Based on the established models, the parametric studies are conducted for linear and nonlinear harvesters. In section 3.1, we tune the mass of the attached linear oscillator to achieve the optimal configuration of the linear 2DOF PEH. In section 3.2, the effects of the magnetic configurations and the parasitic linear oscillator configurations on the performance of the nonlinear 2DOF PEH are investigated and compared with the linear 2DOF counterpart. The parametric study is conducted given the same excitation level of 4 ms^{-2} and the same load resistance R of 1000 kΩ (close to open circuit condition) for

all the cases. In addition, the root mean square (RMS) value is calculated for steady-state voltage response.

3.1 Linear 2DOF Harvester

The reference [7] has demonstrated that the 2DOF PEHs can achieve two significant peaks close to each other by adjusting the system parameters carefully. For a specific 2DOF PEH model as shown in Figure 1, we tune the mass of the oscillator m_2 to achieve this. The following parameters are used for analysis: m_1=0.03715 kg, k_1=4011.716 Nm^{-1}, ζ_1=0.0093, k_2=94 Nm^{-1}, ζ_2=0.0125, θ=0.0005 and C^S=20 nF. The mass m_2 is originally set to be $m_2=m_0$, where m_0=0.003195 kg, and then varied to achieve the optimal configuration. Figure 3(a) shows the open circuit voltage outputs for the original parasitic oscillator configuration of $m_2=m_0$. Two peaks are noted in Figure 3(a). However, because the given parameters are not well-adjusted, they are a bit far away from each other and the first peak has minor contribution to energy harvesting. Then we adjust m_2 to achieve two significant and close resonant peaks. Figure 3(b) shows the voltage outputs of the linear 2DOF PEH for adjusted parasitic oscillator configurations ($m_2=0.25m_0$, $m_2=0.298m_0$, and $m_2=0.333m_0$). It is noted that as m_2 is increased from $0.25m_0$ to $0.333m_0$, the first voltage peak is decreased from 35.1 V to 15.2 V and the second peak is increased from 10.6 V to 27.6 V. For a medium value, $m_2=0.298m_0$, the system gives the closest two peaks, both with significant outputs around 21.5 V. This configuration will be regarded as the optimal linear 2DOF configuration and will be compared with nonlinear 2DOF configurations in the following sections.

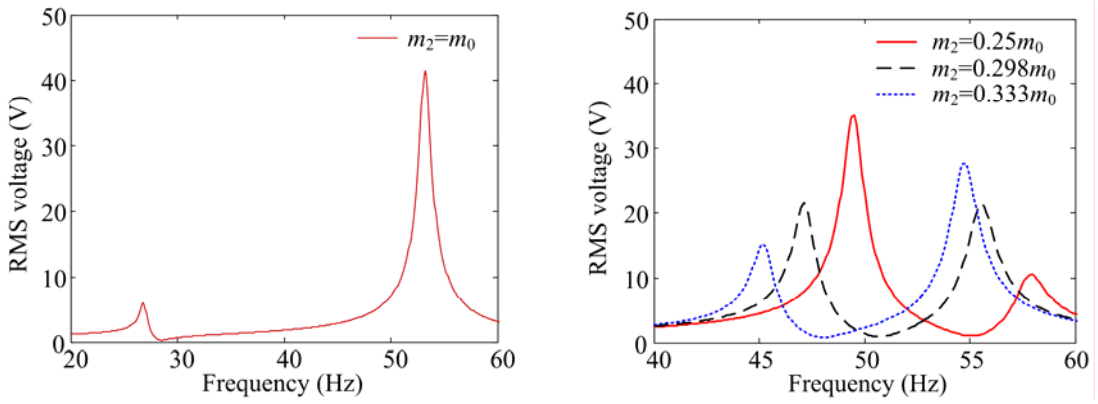

Figure 3. Comparison of voltage outputs for linear 2DOF PEH with (a) original oscillator configuration and (b) adjusted oscillator configurations. m_0=0.003195 kg.

3.2 Nonlinear 2DOF Harvester

In this section, the effects of the magnetic configurations and the parasitic oscillator configurations on the performance of the nonlinear 2DOF PEH are investigated and the nonlinear performance of the system is compared with the linear 2DOF counterpart.

3.2.1 Parametric Study on Magnetic Configuration

Similar to the linear 2DOF PEH, the following parameters are used in the numerical simulation of nonlinear 2DOF PEH, i.e., m_1=0.03715 kg, k_1=4011.716 Nm^{-1}, ζ_1=0.0093, θ=0.0005, C_1=20 nF, m_2=m_0=0.003195 kg, k_2=94 Nm^{-1}, and ζ_2=0.0125. Parameters related to the magnetic force are given as μ_0 =4π×10^{-7} NA^{-2} and σ_1=-σ_2 =0.2 Am^2 (repulsive magnets).

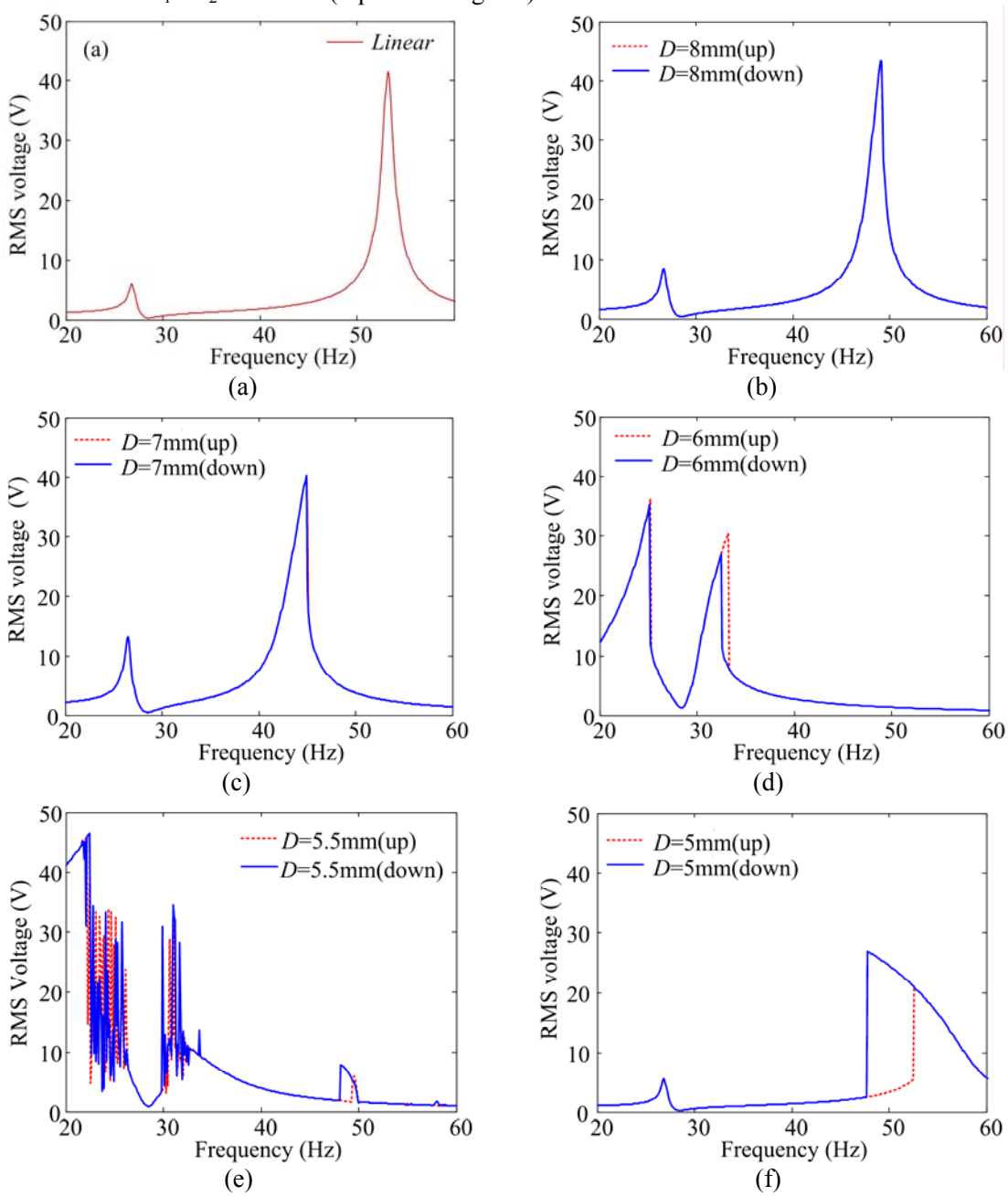

Figure 4. Voltage outputs of (a) linear 2DOF PEH and (b)-(f) nonlinear 2DOF PEH with different magnet configurations. m_2=m_0.

Figure 4 shows voltage outputs from the linear 2DOF PEHs and the nonlinear 2DOF PEHs with different magnetic configurations (adjusting distance D between magnets). Both upward and downward sinusoidal sweeps are performed for each nonlinear configuration. It can be seen from Figures 4(a)-4(d)

that with the appearance of the magnetic coupling and the decrease of D, the first peak slightly moves towards the left while the second peak moves in the same direction but much faster than the first peak. Thus, the nonlinear 2DOF PEH can achieve two resonant peaks close to each other. Meanwhile, it is noted in Figures 4(b) and 4(c) that with a large distance between the two repulsive magnets (D=8 mm and D=7 mm), the response is similar to the linear response and there is no much difference between the upward and downward sweeps. With the further decrease of the distance (D=6 mm), the monostable nonlinear dynamics is observed (Figure 4(d)). The two peaks are bent to the right and upward sweep captures the high energy orbit and downward sweep captures the low energy orbit. More importantly, with the decrease of D, the first peak gradually increases while the second one decreases, and thus both peaks tend to provide significant outputs at D=6 mm. The voltage output is further increased in the lower frequency range with the decrease of the distance between magnets to D=5.5 mm (Figure 4(e)). However, instead of two peaks, chaotic behavior appears when the system is transiting from monostable to bistable status. The transient chaotic response is shown in Figure 5(a). When the distance between the magnets is further reduced to D=5 mm (Figure 4(f)), the system enters bistable status. The first peak is similar to that in the linear case while the second peak is bent to the left associated with the intra-well dynamics providing high energy and low energy orbits according to different sweep directions. Figure 5(b) shows the transient response of the bistable configuration at 50 Hz where the oscillations are confined in potential well (reflected by the fact that m_1 is oscillating about certain negative position).

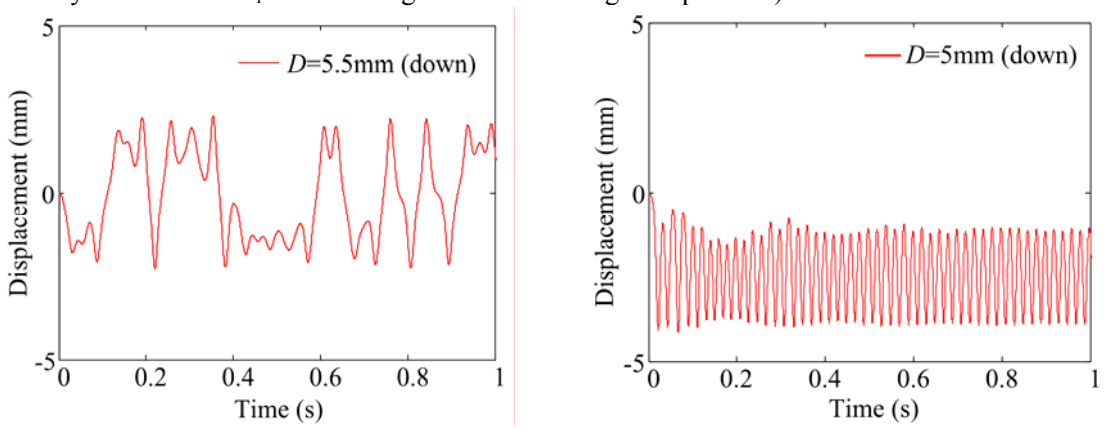

(a) (b)

Figure 5. Transient displacement responses of the mass m_1 for nonlinear 2DOF PEHs for (a) D=5.5 mm at 25 Hz and (b) D=5mm at 50 Hz

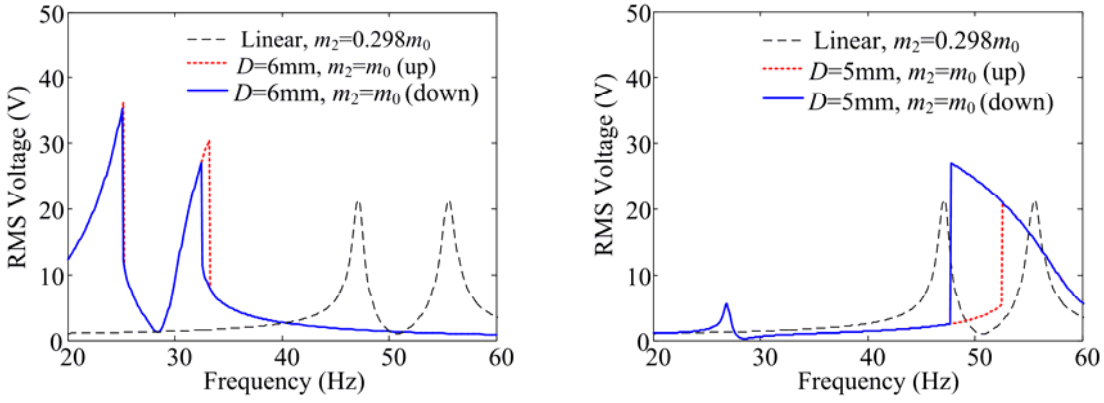

(a) (b)

Figure 6. Comparison of performances between optimal linear 2DOF PEH and (a) monostable (D=6 mm) and (b) bistable (D=5 mm) nonlinear 2DOF PEHs

Figure 6 compares the performances of monostable and bistable nonlinear configurations with the optimal linear case (m_2=0.298m_0 in Figure 3(b)). For the monostable configuration D=6 mm (Figure 6(a)), two resonant peaks are close to each other and both gives significant outputs, which is similar to the linear case. However, this nonlinear configuration is advantageous over the linear case in terms of higher peak outputs of 36.14 V and 30.49 V (around 21.5 V for both peaks in the optimal linear configuration) and widened bandwidth thanks to nonlinear dynamics. For the bistable configuration D=5 mm (Figure 6(b)), though the first peak cannot contribute much to broadband energy harvesting. The bent second peak (especially for downward sweep) also provides higher peak output (27.02 V) and widened bandwidth, though m_1 is confined and only intra-well dynamics is achieved.

3.2.2 Parametric Study on Parasitic Oscillator Configuration

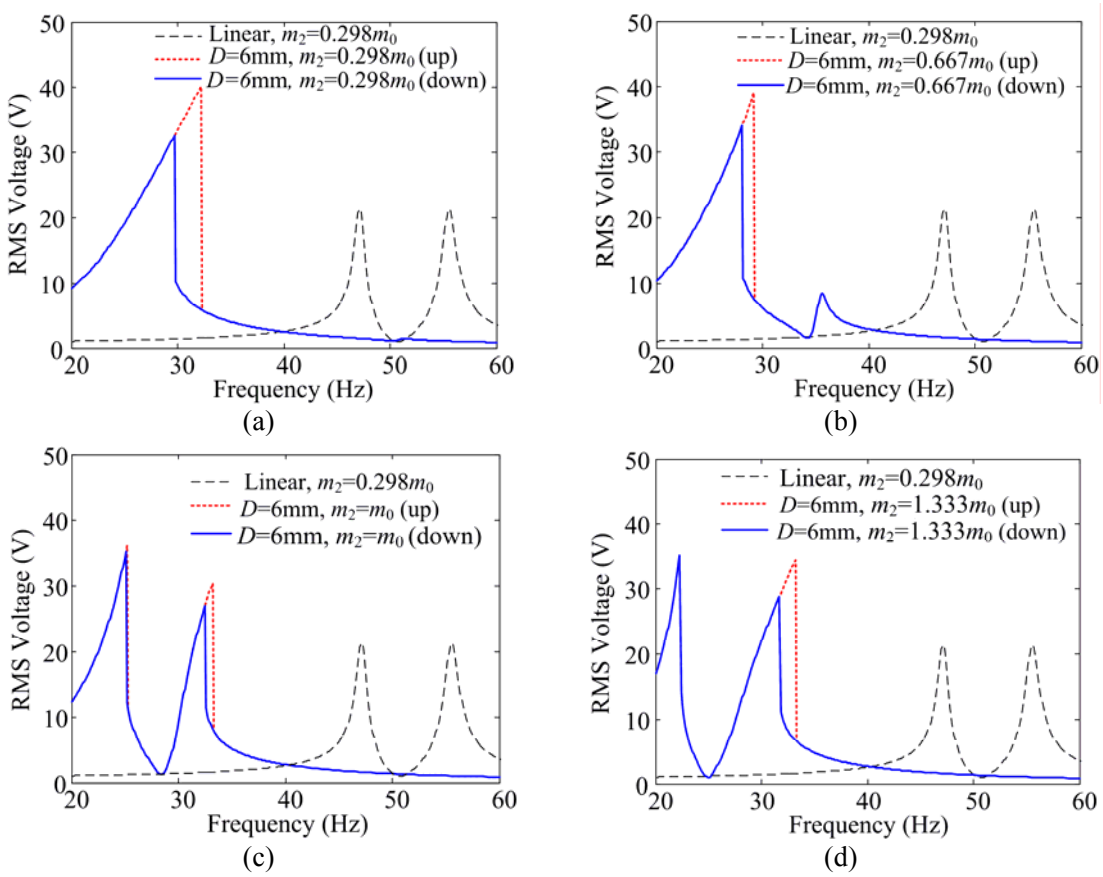

Figure 7. Voltage outputs of nonlinear 2DOF PEHs with different oscillator configurations and comparison to the optimal linear 2DOF PEH

The results in Section 3.2.1 suggest that the magnetic configuration for D=6 mm has the significant advantage of achieving two close significant peaks than other magnetic configurations. In this section, we fix D=6 mm and further analyze the effect of the oscillator configurations on the performance of the nonlinear 2DOF PEH. We keep all the parameters of the nonlinear 2DOF PEH except m_2. Different parasitic linear oscillator configurations are achieved by adjusting m_2.

Figure 7 compare the voltage outputs of the nonlinear 2DOF PEHs with different parasitic oscillator configurations and the optimal linear 2DOF PEH (m_2=0.298m_0). In Figures 7(a)-7(d), the mass of the oscillators are given as m_2=0.298m_0, m_2=0.667m_0, m_2=m_0, m_2=1.333m_0, respectively. It is observed that, in general, with the increase of m_2, the second peak arises associated with the appearance and enhancement of nonlinearity, while the nonlinear dynamic response of the first peak is mitigated (difference between upward and downward sweeps disappears). For two lighter oscillators, m_2=0.298m_0 and m_2=0.667m_0, the second peak has minor contribution to the performance. Though only the first peak contributes to energy harvesting, because of strong nonlinearity and the higher peak outputs, the nonlinear 2DOF PEHs are still advantageous over the linear counterpart. For heavier oscillators, for example, m_2=m_0 and m_2=1.333m_0, two close significant peaks are achieved. Especially, given m_2=1.333m_0, two peak voltage outputs of 35.06 V and 34.06 V are achieved, together with the widened bandwidth thanks to the enhanced nonlinear dynamics at the second peak. This is much more advantageous over the optimal linear 2DOF PEH.

4. CONCLUSIONS

To broaden the bandwidth of the vibration energy harvester, this paper proposes a nonlinear 2DOF PEH with magnetic coupling. An electromechanical model for the nonlinear 2DOF PEH is established. Parametric studies are conducted on various repulsive magnetic configurations and parasitic oscillator configurations. The results show that the enhanced magnetic coupling can induce monostable, chaotic and bistable behaviors of the 2DOF PEHs. In the monostable configuration, the system can be tuned to have two close significant peak outputs associated with strong nonlinear dynamics. The peak outputs of the tuned monostable configuration are higher than the optimal linear 2DOF PEH and wider bandwidth is achieved thanks to the nonlinearity. In the bistable configuration, though there might be only one peak contributing to energy harvesting and the system is confined for intra-well oscillations, the higher peak output and wider bandwidth due to nonlinearity than the linear counterpart are still attractive.

ACKNOWLEDGMENTS

This work is supported by Department of Mechanical Engineering in University of Auckland and Young Teacher's Scientific Research Program in Qiqihar University (2012k-Z12).

REFERENCES

1. Erturk, A., Renno, J.M., Inman, D.J., "Modeling of Piezoelectric Energy Harvesting from an L-Shaped Beam Mass Structure with an Application to UAVs," *Journal of Intelligent Material Systems and Structures*, Vol. 20, No. 5, 2009, pp. 529 -544.
2. Wu, H., Tang, L., Yang, Y., Soh, C.K., "A Compact 2 Degree-of-Freedom Energy Harvester with Cut-out Cantilever Beam," *Japanese Journal of Applied Physics*, Vol. 51, No. 4R, 2012, 040211.
3. Wang, H., Tang, L., Guo, Y., Shan, X., Xie, T., "A 2DOF Hybrid Energy Harvester based on Combined Piezoelectric and Electromagnetic Conversion Mechanisms," *Journal of Zhejiang University SCIENCE A*, Vol. 15, No. 9, 2014, pp. 711-722.
4. Aldraihem, O., Baz, A., "Energy Harvester with Dynamic Magnifier," *Journal of Intelligent Material Systems and Structures*, Vol. 22, No. 6, 2011, pp. 521-530.

5. Ali, S.F., Adhikari, S., "Energy Harvesting Dynamic Vibration Absorbers," *Journal of Applied Mechanics*, Vol. 80, No. 4, 2013, 041004.
6. Harne, R.L., "Theoretical Investigations of Energy Harvesting Efficiency from Structural Vibrations using Piezoelectric and Electromagnetic Oscillators," *The Journal of the Acoustical Society of America*, Vol. 132, No. 1, 2012, pp. 162-172.
7. Tang, L., Yang, Y., Wu, H., "Modeling and Experiment of A Multiple-DOF Piezoelectric Energy Harvester," *SPIE Smart Structures/NDE*, Vol. 8341, 83411E, San Diego, CA, USA, 2012.
8. Tang, X., Zuo, L., "Enhanced Vibration Energy Harvesting using Dual-Mass Systems," *Journal of Sound and Vibration*. Vol. 330, No. 21, 2011, pp. 5199-5209.
9. Ou, Q., Chen, X., Gutschmidt, S., Wood, A., Leigh, N., Arrieta, A.F., "An Experimentally Validated Double-Mass Piezoelectric Cantilever Model for Broadband Vibration-Based Energy Harvesting," *Journal of Intelligent Material Systems and Structures*. Vol. 23, No. 2, 2012, pp. 117-125.
10. Castagnetti, D. "Experimental Modal Analysis of Fractal-Inspired Multi-Frequency Structures for Piezoelectric Energy Converters," *Smart Materials and Structures*, Vol. 21, No. 9, 2012, 094009.
11. El-Hebeary, M.M.R., Mustafa, H.A., Said, M.M., "Modeling and Experimental Verification of Multi-Modal Vibration Energy Harvesting from Plate Structures," *Sensors and Actuators A: Physical*, Vol. 193, 2013, pp. 35-47.
12. Stanton, S.C., McGehee, C.C., Mann, B.P., "Nonlinear Dynamics for Broadband Energy Harvesting: Investigation of a Bistable Piezoelectric Inertial Generator," *Physica D: Nonlinear Phenomena*. Vol. 239, No. 10, 2010, pp. 640-653.
13. Erturk, A., Hoffmann, J., Inman, D.J., "A Piezomagnetoelastic Structure for Broadband Vibration Energy Harvesting," *Applied Physics Letters*, Vol. 94, No. 25, 2009, 254102.
14. Tang, L., Yang, Y., Soh, C. K., "Improving Functionality of Vibration Energy Harvesters using Magnets," *Journal of Intelligent Material Systems and Structures*, Vol. 23, No. 13, 2012, pp. 1433-1449.